ADVANCED MATERIALS INTERFACES
www.advmatinterfaces.de

Effects of Temperature on the Tribovoltaic Effect at Liquid-Solid Interfaces

*Mingli Zheng, Shiquan Lin, Laipan Zhu, Zhen Tang, and Zhong Lin Wang**

Energy harvesters based on tribovoltaic effect are interesting due to their direct current output characteristic that matches most commercial electronic devices. However, their mechanism remains to be further investigated, especially for liquid-solid cases. Here, the effect of temperature on the tribovoltaic effect at liquid-solid interfaces is studied. The results show that the increasing of temperature will lead to the increase of the tribo-voltage and tribo-current at the water/Si and water/metal interfaces during sliding. Moreover, the coupling effect of the pH value of the liquid and the temperature on the tribovoltaic effect is demonstrated, and an energy band model is proposed for understanding the received data, in which the energy released ("bindington") by contacting the liquid and the solid with the formation of chemical bonds is considered to be responsible for the generation of tribovoltaic effect.

1. Introduction

Energy harvesters based on tribovoltaic effect have attracted wide attention due to their direct current output characteristic which can match most commercial devices.[1–8] The tribovoltaic effect exists in the process of sliding between semiconductor and semiconductor (liquid or metal), in which the direct current generation is essentially different from that in traditional DC output triboelectric nanogenerator (TENG) with circuit management[9–13] or special structure.[14–17] However, the mechanisms of tribovoltaic effect are still under debate,[18–24] especially for liquid-solid cases.[23,24] In our previous studies, a concept of "bindington," which denotes the energy released due to the formation of the bonds at the interfaces during contact or sliding, has been first proposed.[24] The "bindington" further excites the electron-hole pairs, leading to the generation of tribo-current. Though the concept of "bindington" successfully explains the tribovoltaic effect, it is still necessary to find more experimental evidences to support this proposal.

The temperature significantly changes the energy band structure and surface characteristics of semiconductors, which has been extensively explored in the studies related to photovoltaic[25,26] and the catalysis.[27,28] It has been demonstrated that the Seebeck effect increase the tribo-current and tribo-voltage of the tribovoltaic effect for the semiconductor/semiconductor case.[29] On the other hand, it's well known that the chemical reaction rate at the liquid-solid interface is highly dependent on the temperature, which implies that the temperature is an important factor affecting the bonding rate at the interface.[30] According to the concept of "bindington," an expected result is that temperature will have an important influence on the rate of "bindington" formation and further affect the output of tribo-voltage and tribo-current at liquid-semiconductor interface. Therefore, a thorough study of the effect of temperature on the tribovoltaic effect at liquid/semiconductor is helpful to clarify the mechanism of tribovoltaic effect and verify the concept of "bindington."

Here, the effect of temperature on the tribovoltaic effect at the liquid and semiconductor has been demonstrated. The results show that the direct tribo-current and tribo-voltage are generated at the water/Si and water/metal interfaces during sliding, and the increasing of temperature will lead to the increase of the tribo-voltage and tribo-current. The coupling effect of the pH value of liquid and temperature on the tribovoltaic effect was investigated, and an energy band model was proposed, in which the energy released ("bindington") generated at the liquid-solid interface during in forming chemical bonds is responsible for the generation of tribovoltaic effect. Moreover, the findings may have implications in the field of low-grade heat energy conversion and solid-liquid triboelectric nanogenerator.

2. Results and Discussion

The effects of the temperature on the tribo-current and tirbo-voltage at the deionized water (DI water) and the Si wafer

M. Zheng, S. Lin, L. Zhu, Z. Tang, Z. L. Wang
Beijing Institute of Nanoenergy and Nanosystems
Chinese Academy of Sciences
Beijing 101400, P. R. China
M. Zheng, S. Lin, L. Zhu, Z. Tang, Z. L. Wang
School of Nanoscience and Technology
University of Chinese Academy of Sciences
Beijing 100049, P. R. China
Z. L. Wang
CUSTech Institute
Wenzhou, Zhejiang 325024, P. R. China
Z. L. Wang
School of Materials Science and Engineering
Georgia Institute of Technology
Atlanta, GA 30332-0245, USA
E-mail: zlwang@gatech.edu

The ORCID identification number(s) for the author(s) of this article can be found under https://doi.org/10.1002/admi.202101757.

DOI: 10.1002/admi.202101757

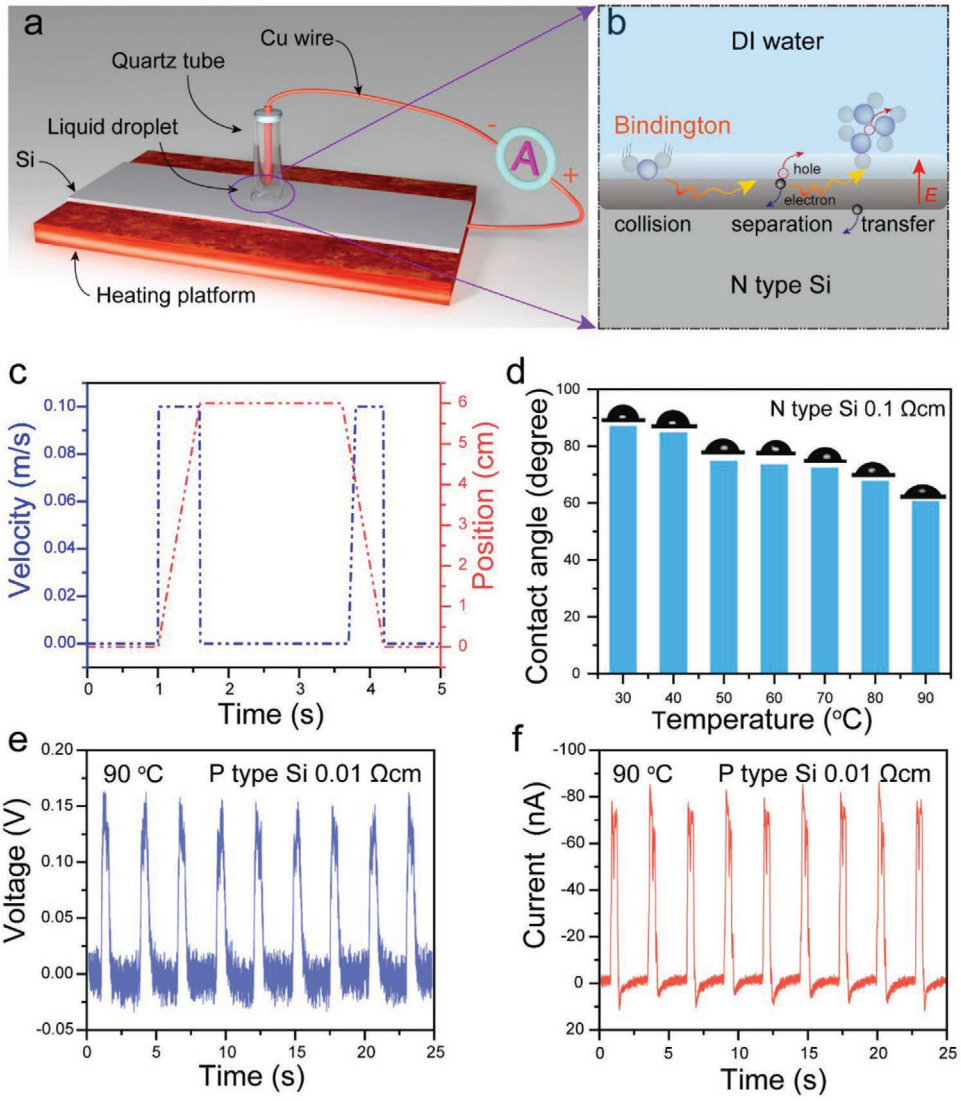

Figure 1. The experiment setup and the tribovoltaic effect at the DI water and the Si interface. a) The setup of the experiments. b) A schematic diagram of the generation of tribo-current. c) The relative position and velocity between the Si wafer and the DI water droplet. d) The change of contact angle between Si (N-type 0.1 Ω cm) and water with temperature rising. The e) tribo-voltage and the f) tribo-current when a DI water droplet slides on the P-type Si (0.1 Ω cm) surface at 90 °C.

interface were investigated. The Si wafer was placed in an immobile heating platform and a quartz tube with a Cu electrode was mounted on a mobile holder, as shown in **Figure 1**a. In order to eliminate the noise generated by the heating table during the test, the heating table was first raised to 95 °C, and the output of tribo-current was tested under different temperature during the cooling process after the power was turned off. The temperature of Si/DI water interface was determined by an infrared camera. In the experiment, the Cu wire contacted with the DI water. The tribo-current and the tribo-voltage (or called as the open-circuit voltage and the short-circuit current) were measured by using electrometer (Keithley 6514). The external tribo-voltage and tribo-current from the Si wafer side to the DI water droplet side are defined as positive. Figure 1b gives the schematic diagram of tribo-current generation induced by the tribovoltaic effect. When a water molecule collides with the atoms belonging to the Si surface, the energy will be released due to the formed bond at the interface, named as "bindington." Then, an electrons-hole pair will be excited by a "bindington" and separated by the built-in electric field at the DI water and Si interface. The electrons and holes transfer to the N-type Si side and water side, respectively. Here, a hole may be shared by several water molecules or clusters, instead of belonging to one molecule.[31,32] Figure 1c gives the velocity and displacement curve of the water droplet sliding on the Si wafer. The contact angle of water and N type Si wafer (the resistivity: 0.1 Ω cm) at different temperatures was demonstrated in Figure 1d. It clearly illustrates that the contact angle decreased from 86.72° to 60.36° with the temperature rising from 30 to 90 °C. During the DI water sliding on the Si surface at different temperature, the temperature in the interface of water droplet and Si wafer was not different in the infrared

camera picture as shown in Figure S1 (Supporting Information), which excludes the Seebeck effect on the experiments.[29] The I-V curve of different Si wafer with aluminum electrode vapor deposited on the back was shown in Figure S2 (Supporting Information), revealing that the resistivity of the Si wafer hardly changes with the temperature rising in the range of 30–90 °C. It should be noted that there is a Schottky barrier between the N-type Si wafer (resistivity: 0.01 and 0.1 Ω cm) and the aluminum electrode, but the height of the Schottky barrier does not change with temperature implies that little impact on subsequent experimental results. In the experiment, a water column about 1.0 cm length is sealed under the balance of gravity and capillary action in the tube which one end closed by silica gel. This structure has the ability to replenish the evaporated water in time resulting a stable output during the DI water droplet sliding on the Si wafer surface at high temperature, as shown in Movie S1 (Supporting Information). We excluded the water evaporation contribute to electricity generation because that the external circuit is connected in different ways between the hydrovoltaic effect and the tribovoltaic effect, where in the hydrovoltaic effect two electrodes are connected to the solid surface,[33,34] while one electrode is connected to the liquid side and the other electrode is connected to the solid side for collecting tribovoltaic current. Figure 1e,f gives the tribo-voltage and tribo-current of the tribovoltaic effect between P type Si (resistivity: 0.01 Ω cm) and DI water at 90 °C, which are stable in 9 output cycles and achieve to 0.15 V and 70 nA, respectively.

The effects of temperature on the tribovoltaic effect at the N-type Si and the DI water interface have been investigated. The I-V curves of the N-type Si wafers with different resistivity and the DI water are shown in Figure S2 (Supporting Information). With the increasing of the Si resistivity and the temperature, the reverse current of the I-V curve increases, indicating that there is a depletion region at the interface of the water droplet/Si and the width of the depletion region and the intensity of the built-in electric field are closely related to the resistivity of N-type Si and the temperature. **Figure 2** gives the tribo-voltage and tribo-current of DI water droplet sliding at the surface of N-type Si wafer with different resistivity. The direction of the tribo-current and tribo-voltage in the external circuit is from the water droplet side to the N-type Si wafer side. The results are consistent with that of the tribovoltaic effect, in which the external tribo-current is considered to be depended on the direction of built-in electric field. For high resistivity Si (1 Ω cm), the tribo-voltage increases with the temperature rising, as shown in Figure 2a. The tribo-voltage increases from 0.1 to about 0.4 V increasing about 0.3 V, when the temperature rises from 30 to 90 °C. This result is contrary to the change of open-circuit voltage with temperature rising in the photovoltaic

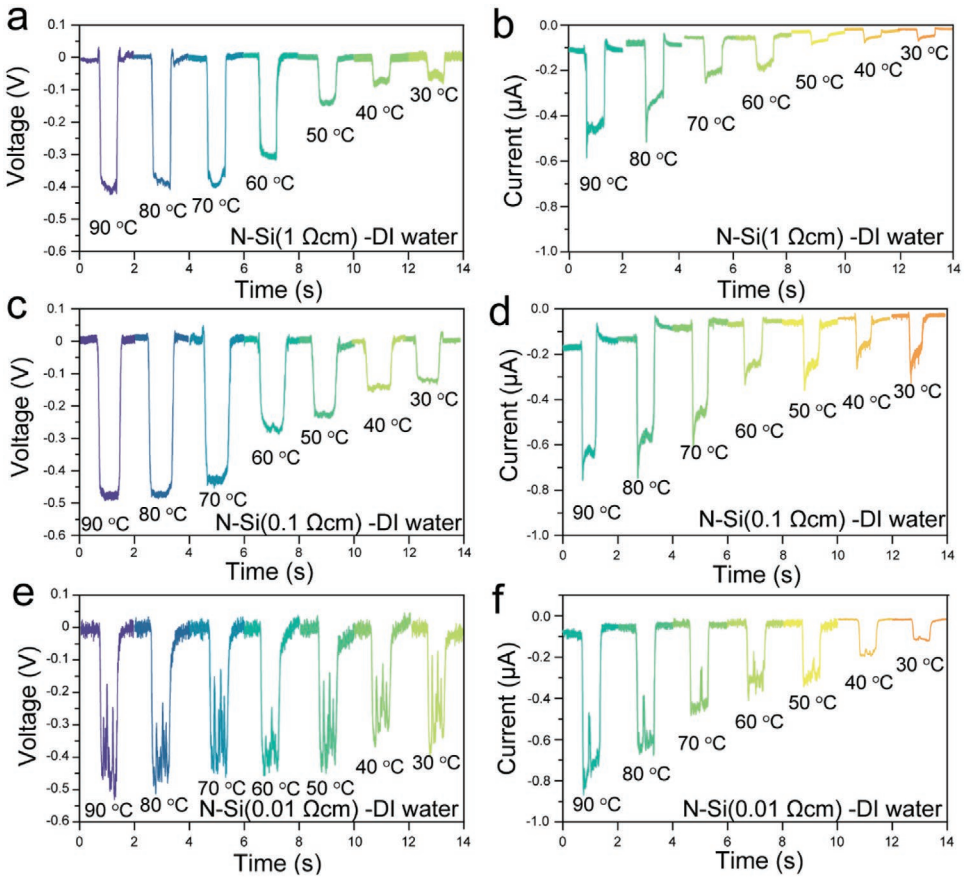

Figure 2. Effect of temperature on the tribovoltaic effect at N-type Si and DI water interfaces. a,c, e) The tribo-voltage and b,d,f) the tribo-current when a DI water droplet slides on N-type Si (1, 0.1, and 0.1 Ω cm) surface at different temperature.

effect, in which the open-circuit voltage decreases with the rising of temperature mainly because of the temperature increasing the intrinsic carrier concentration of Si, reducing the strength of the inner built electric field.[25,26] It should be noted that the changed amount of the tribo-voltage decreases with temperature rising for low resistivity Si. For example, the tribo-voltage between the DI water and the N-type Si with 0.01 Ω cm increases from 0.35 V at 30 °C to about 0.5 V at 90 °C, which increase about 0.15 V less than that of the DI water and the N-type Si with 1 Ω cm, as shown in Figure 2e. This result should be closely related to the band structure of the Si with different resistivity and the water interface because of a logarithmic relationship between carrier concentration and Fermi level. For the tribo-current (or the short-circuit current), there is a dark current about 0.1 μA among the three kinds resistivity of Si and water at 90 °C, as shown in Figure 2b,d,f. The reason should be that the electron-hole pairs excited by the high temperature and separated in the built-in electric field at the interface of Si and DI water forming a thermal current, which once again verifies the correctness of the tribovoltaic effect. The tribo-current of the three kinds resistivity of N-type Si also increases with temperature rising. The change of the tribo-current with the temperature rising is unlikely to be caused only by the change of resistivity of the Si or the water with temperature. The equivalent ohmic resistance at −3 V bias is regarded as the resistance of water and Si, which is considered as internal resistance in the tribo-voltaic effect. The resistivity of equivalent ohmic resistance changes at 30 and 90 °C less than twice while the tribo-current increases about fourfold in sliding process for N-type Si with 0.01 Ω cm and DI water case. Therefore, the tribo-current should be closely related to the concentration of excited carriers. In the tribovoltaic effect, the charge carriers are mainly excited by the "bindingtons" and separated by the built-in electric field at the interface of Si/DI water.[35,36] The experimental results suggest that the generating rate of "bindington" increasing as the temperature rising should be the mainly reason of the increasing tribo-current.

The outputs of the tribo-current and tribo-voltage at the P-type Si and the DI water interface are also studied. The I-V curves of P-type Si/water/Cu are shown in Figure S4a–c (Supporting Information). The I-V curves of high resistivity Si show a good rectification characteristic at room temperature (30 °C), shown as Figure S4a,b (Supporting Information), indicating that there is a depletion zone at the interface of the P-type Si and the DI water. Figure S4c (Supporting Information) gives that the I-V curve is nonlinear showing back-to-back Schottky barrier transport characteristics at room temperature. The current under positive and negative bias is closely related to the Si/water and water/Cu interface barrier.[37] Figure S4d (Supporting Information) gives the energy band structure of P-type Si/water/copper. The tribo-current and tribo-voltage at the interface between the water droplet and the P-type Si are shown in **Figure 3**. The external circuit direction of tribo-voltage and tribo-current is from the P-type Si wafer side to the water droplet side, since that the direction of the built-in electric field at the interface is pointing from the water side to the P-type Si side. The tribo-voltage of tribovoltaic effect between the P-type Si with the resistivity of 0.01 Ω cm and the DI water increased from 0.1 V at 30 °C to 0.16 V at 90 °C as shown in Figure 3e. When water slides on the N-type Si wafer (0.01 Ω cm) in the experiment, very small water droplets will remain on the Si surface, which will be no output of tribo-voltage between these residual water droplets and water, leading a combination spike. The tribo-current increases from 30 nA at 30 °C to 75 nA at 90 °C as shown in Figure 3f. It should be noted that the dark current of the P-type Si and water interface is very small at high temperature (90 °C) compared with the dark current of N-type Si and water interface. It should be related to the effective mass of carriers in different type Si wafer, where the effective mass of hole is much higher than electron resulting in a smaller mobility.

The I-V curves of P-type Si/water/copper in Figure S3 (Supporting Information) indicate that there is depletion region at the metal/water interface, so that it is highly suspected that tribovoltaic effect may also exist at the metal and water interface. The tribovoltaic effect at the Au/water and the Pt/water interfaces has been studied because of the stable chemical property of Au and Pt without oxide layer on the surface. The I-V curves are not linear as shown in Figure S5 (Supporting Information), indicating that there is a depletion region at the Au or Pt and water interface. During water sliding on the Au or Pt surface, the direction of tribo-voltage and tribo-current in the external circuit is positive, which is from the metal side to the droplet water, as shown in **Figure 4**. The tribo-voltage at the interface of Au/water and Pt/water are only about 20 mV at room temperature (30 °C) as shown in **Figures 4**a,c, which may be the reason why the tribovoltaic effect of metal and water interface has been neglected for a long time. With the temperature rising, the tribo-voltage of tribovoltaic effect between two metals and water increases to 58 mV and 68 mV at 90 °C, respectively. These results are consistent with the effects of temperature on the tribo-voltage at Si and water interface. The tribo-current of Au/water and Pt/water increases with the temperature rising as same as that of Si and water. It should be pay attention to that the dark current of Pt/water is as high as 120 nA in the quiescent state, which is related to the decomposition of water molecules catalyzed by Pt.[38] It should be pointed out that the change of metal resistivity is very limited in the range of 30–90 °C. Meanwhile, the relevant literatures show that the changes of water resistivity and water clusters are also very little in this temperature range.[39,40] Therefore, the increase of tribo-current is not only caused by the change in resistivity of water and metal, but mainly related to the change of carrier concentration excited by the "bindington" with the temperature rising. The foreseeable reason that the changes of open-circuit voltage with temperature rising in the tribovoltaic effect at Si (or metal) and water inconsistent with that of in photovoltaic effect should be closely related to the change of carrier concentration excited by the "bindington."

One needs to notice is that the variation of tribo-voltage between NaOH and Si wafer with temperature is closely related to the pH value. Here, the resistivity of N-type Si is 0.01 Ω cm. For the weak alkaline solution with pH value of 9, the tribo-voltage of tribovoltaic effect also increases with the temperature rising, from 0.25 V at 30 °C to 0.35 V at 90 °C, as shown in **Figure 5**a. The tribo-current increases with the temperature rising as same as that of DI water/Si (or metal), and the dark current at 90 °C is about 180 nA, as shown in Figure 5b. When

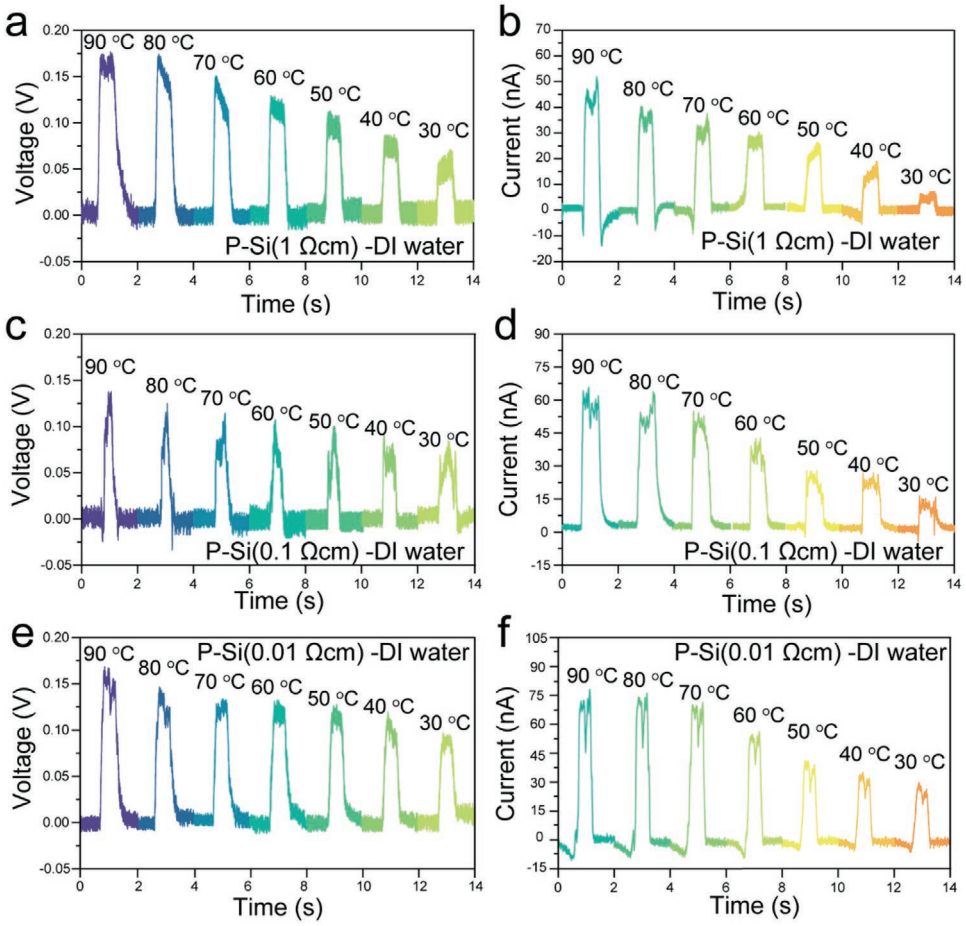

Figure 3. Effect of temperature on the tribovoltaic effect at P-type Si and DI water interfaces. a,c,e) The tribo-voltage and b,d,f) the tribo-current when a DI water droplet slides on P-type Si (1, 0.1, and 0.1 Ω cm) surface at different temperature.

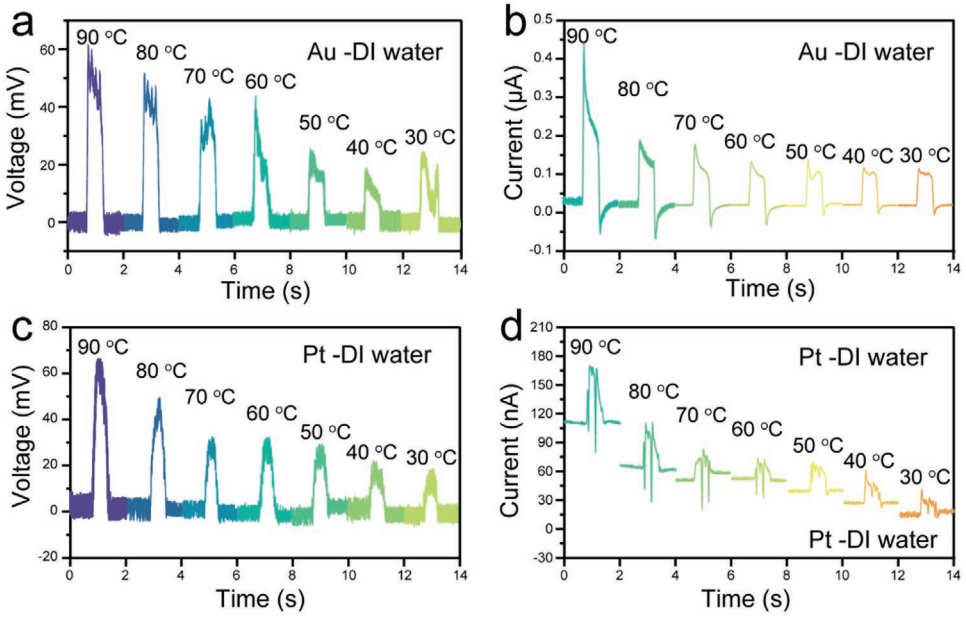

Figure 4. Effect of temperature on the tribovoltaic effect at metal and DI water interfaces. a,c) The tribo-voltage and b,d) the tribo-current when a DI water droplet slides on Au or Pt surface at different temperature.

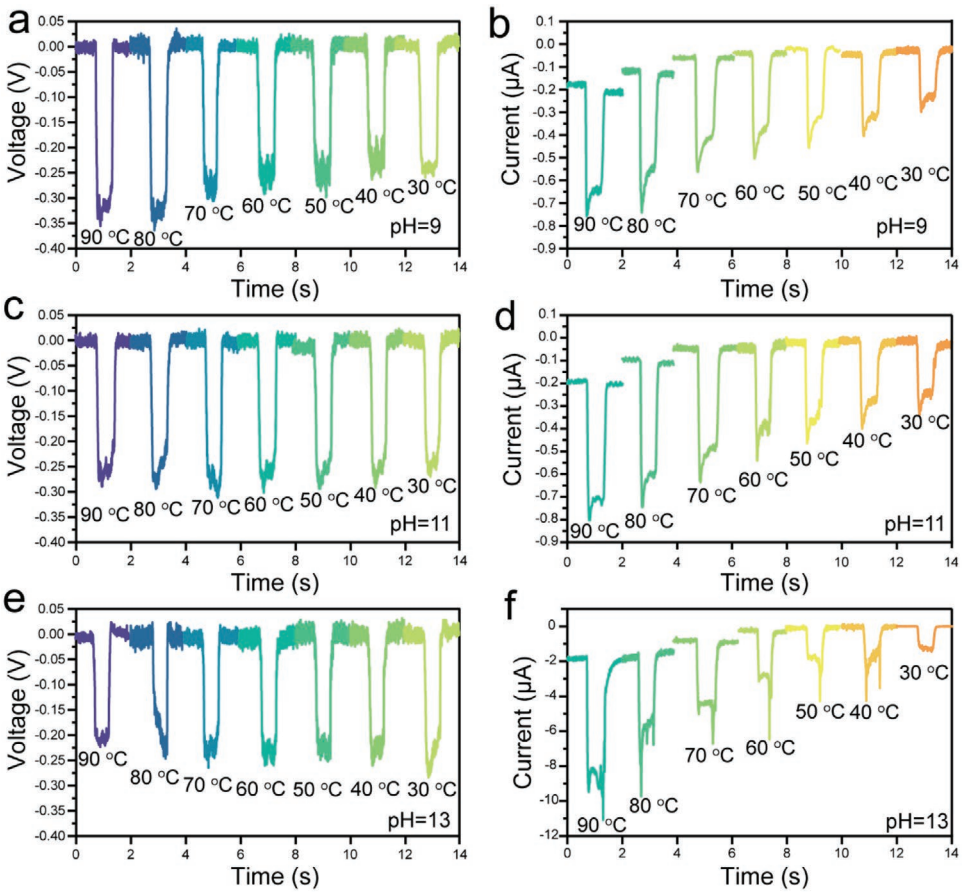

Figure 5. Effect of temperature on the tribovoltaic effect at N-type Si and NaOH solution interfaces. a,c,e) The tribo-voltage and b,d,f) the tribo-current when a NaOH solution droplet (pH = 9, 11, and 13) slides on P-type Si (0.1 Ω cm) surface at different temperature.

the pH value is 11, the tribo-voltage of tribovoltaic effect does almost not change with temperature rising shown in Figure 5c. The tribo-current still increases with temperature rising and the dark current at 90 °C are about 200 nA, as shown in Figure 5d. However, when the pH value is 13, the change of the open-circuit voltage of the tribovoltaic effect with the temperature is similar to that of the photovoltaic effect, which decrease from 0.25 to 0.20 V with the temperature rising from 30 to 90 °C shown in Figure 5e. It should be noted that when the pH value is 13, the dark current and the tribo-current are as high as about 2 and 8.5 μA at 90 °C respectively as shown in Figure 5f. This indicates that the redox reaction of NaOH solution and Si apparently increases the concentration of excited carriers including the intrinsic carrier. In the photovoltaic effect, the intrinsic carrier concentration increases exponentially with the temperature rising, which reduces the open-circuit voltage of the photovoltaic effect. So that these results should not be caused by the increase of intrinsic carrier concentration excited by the redox reaction of NaOH solution and Si. The "bindington" is defined as the energy released by the bond formation at the interface.[24] Hence, the energy released by redox reactions between NaOH solution and Si interface should be also classified as the "bindington." Higher concentration of OH^- and higher temperature aggravate the generation rate of "bindington" and released a larger amount of thermal energy in the process of redox reaction increasing the intrinsic carrier concentration. Consequently, the effect of temperature on the open-circuit voltage of tribovoltaic effect is consistent with that of the photovoltaic effect.

Based on the experimental data, we propose a model to explain temperature effects on the tribovoltaic effect between semiconductor (or metal) and water, in which the "bindington" plays an important role. The band structure of the N-type Si and the DI water before sliding is shown in **Figure 6**a. When a DI water droplet contacts the surface of N-type Si, the electrons will diffuse from Si side to DI water side and the built-in electric field will be established, as shown in Figure 6b. Meanwhile, a "bindington" will be released at the DI water and the Si interface and excite an electron-hole pair at the sliding process, as shown in Figure 6c. At low temperature, the electron-hole pairs excited by the "bindington" are separated by the built-in electric field, and the electrons transfer into the N-type Si, which raises the Fermi level and produces an open-circuit voltage V as shown in Figure 6d, forming a stable DC output in the external circuit. The resistivity of Si (shown in Figure S2, Supporting Information) and the change of molecule clusters or ionization product constant of water[39] can be ignored in the temperature range of 30–90 °C. With the temperature rising, the increase of tribo-current indicates that the excited carrier concentration is increased significantly, implied that the change of the excited carrier concentration is closely related to the rate

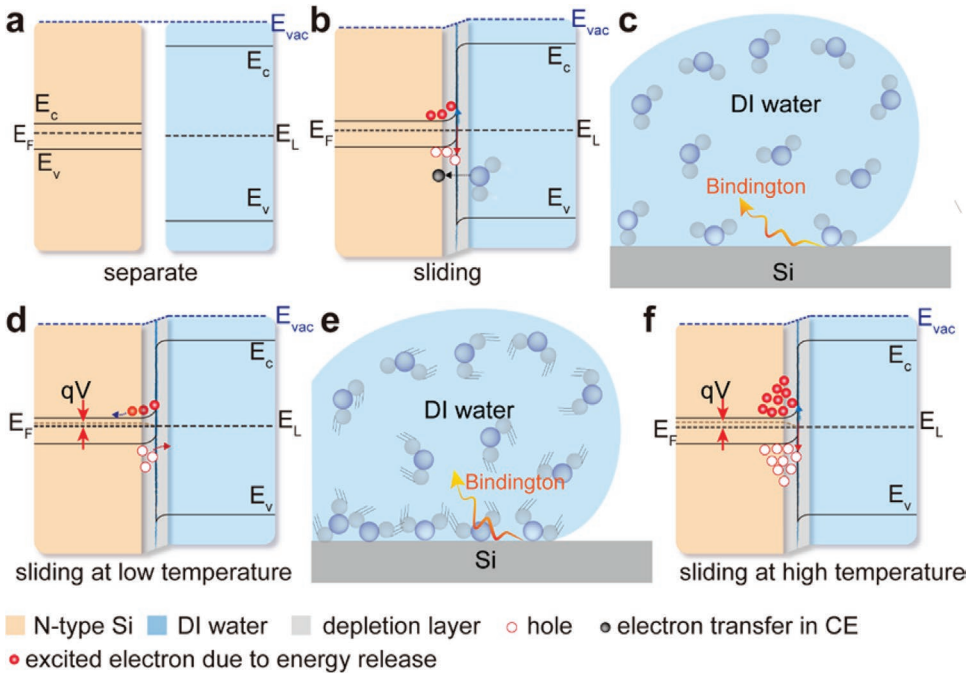

Figure 6. Energy band diagram of the effect of temperature on the tribovoltaic effect. Energy band diagram of the N-type Si and the DI water a) before sliding, b) contact and sliding, at c) low temperature and d) sliding at low temperature, and e) high temperature f) sliding at high temperature. A schematic diagram of the generation of "bindington". (E_c is the bottom of the conduction band, E_f is the Fermi level of the N-type Si, E_L is the "Fermi level" of the DI water and E_v is the top of the valence band. V is the tribo-voltage).

of "bindington" generation. The momentum and the collision number of water molecules should be significantly increased as the temperature rising[41,42] at the interface of the DI water/Si. The electron clouds of the atoms belonging to the DI water and the Si become more likely to overlap with each other at a higher temperature, resulting in the increasing of the "bindington" generation rate, as shown in Figure 6e. Therefore, a mass of excited electron-hole pairs is separated by the built-in electric field, and then electrons transfer into N-type Si side, raising the Fermi level of Si and forming a larger open-circuit voltage V, as shown in Figure 6f. Because the tribovoltaic effect is analogous to the photovoltaic effect, here the formula of open-circuit voltage in the photovoltaic effect is applied to explain the increasing of the tribo-voltaic with increasing temperature[25]:

$$V_{OC} = \frac{mKT}{q} \ln\left(\frac{J_{SC}}{J_m^0} + 1\right) \quad (1)$$

where J_{SC} is the tribo-current, J_m^0 is the current of reverse saturated non ideal diode, T is the temperature, and K is the Boltzmann constant. The open-circuit voltage will increase with temperature rising. The energy band diagram of P-type Si contacting with DI water is also given in Figure S6 (Supporting Information).

3. Conclusions

In conclusion, the effects of temperature on the tribovoltaic effect at the liquid and semiconductor (or metal) interfaces have been demonstrated. It is revealed that the tribo-voltage and tribo-current of the tribovoltaic effect at water/Si and water/metal increase with temperature rising, in which the influence of temperature on the open-circuit voltage is opposite to that of the photovoltaic effect. Moreover, based on the experiment results, an energy band model was proposed to explain the effect of temperature on the tribovoltaic effect at liquid and semiconductor interface, in which a higher temperature leads to a higher "bindington" generation rate. A higher "bindington" generation rate excites more electron-hole pairs and then increase the excited carrier concentration, which affects the electrical output of tribovoltaic effect. Our findings support the concept of "bindington" in the tribovoltaic effect and also provide a novel idea for improving the output performance of the energy harvesters based on the tribovoltaic effect.

4. Experimental Section

Sample Preparation: The P-type Si is boron-doped and the N-type Si is phosphorus-doped resistivity. The aluminum electrode was grown on the back of Si wafer through magnetron sputtering and annealed in a nitrogen atmosphere at 500 °C. The DI water was produced by a deionizer (Hitech, China), and the resistivity of the DI water used here was 18.2 MΩ cm. The Au and Pt were grown on SiO_2 substrate by magnetron sputtering with a thickness of 100 nm.

Current-Voltage Measurements: The current-voltage curves were measured by an electrochemical workstation (CHI600E, China). The scan rate was set to be 0.1 V s^{-1}, the sample interval was 0.001 V.

Supporting Information

Supporting Information is available from the Wiley Online Library or from the author.

Acknowledgements

M.Z. and S.L. contributed equally to this work. This work was supported by the National Key R & D Project from Minister of Science and Technology (2016YFA0202704), National Natural Science Foundation of China (Grant No. 52005044).

Conflict of Interest

The authors declare no conflict of interest.

Data Availability Statement

Research data are not shared.

Keywords

contact electrification, electron transfer, liquid-solid interface, semiconductors, tribovoltaic effect

Received: September 13, 2021
Revised: October 28, 2021
Published online:

[1] J. Liu, A. Goswami, K. Jiang, F. Khan, S. Kim, R. McGee, Z. Li, Z. Hu, J. Lee, T. Thundat, *Nat. Nanotechnol.* **2018**, *13*, 112.
[2] M. Zheng, S. Lin, L. Xu, L. Zhu, Z. L. Wang, *Adv. Mater.* **2020**, *32*, 2000928.
[3] S. Lin, Y. Lu, S. Feng, Z. Hao, Y. Yan, *Adv. Mater.* **2019**, *31*, 1804398.
[4] J. Meng, Z. H. Guo, C. Pan, L. Wang, C. Chang, L. Li, X. Pu, Z. L. Wang, *ACS Energy Lett.* **2021**, *6*, 2442.
[5] Z. Zhang, D. Jiang, J. Zhao, G. Liu, T. Bu, C. Zhang, Z. L. Wang, *Adv. Energy Mater.* **2020**, *10*, 1903713.
[6] M. Kumar, J. Lim, J. Y. Park, H. C. Seo, *Small Methods* **2021**, *5*, 2100342.
[7] A. Šutka, M. Zubkins, A. Linarts, L. Lapčinskis, K. Mālnieks, O. Verners, A. Sarakovskis, R. Grzibovskis, J. Gabrusenoks, E. Strods, K. Smits, V. Vibornijs, L. Bikse, J. Purans, *J. Phys. Chem. C* **2021**, *125*, 14212.
[8] Y. Wang, G. Zhang, H. Wu, B. Sun, *Adv. Energy Mater.* **2021**, *11*, 2100578.
[9] F. Xi, Y. Pang, W. Li, T. Jiang, L. Zhang, T. Guo, G. Liu, C. Zhang, Z. L. Wang, *Nano Energy* **2017**, *37*, 168.
[10] X. Cheng, L. Miao, Y. Song, Z. Su, H. Chen, X. Chen, J. Zhang, H. Zhang, *Nano Energy* **2017**, *38*, 438.
[11] Y. Song, H. Wang, X. Cheng, G. Li, X. Chen, H. Chen, L. Miao, X. Zhang, H. Zhang, *Nano Energy* **2019**, *55*, 29.
[12] W. Shang, G. Gu, W. Zhang, H. Luo, T. Wang, B. Zhang, J. Guo, P. Cui, F. Yang, G. Cheng, Z. Du, *Nano Energy* **2021**, *82*, 105725.
[13] H. Qin, G. Gu, W. Shang, H. Luo, W. Zhang, P. Cui, B. Zhang, J. Guo, G. Cheng, Z. Du, *Nano Energy* **2020**, *68*, 104372.
[14] J. Luo, L. Xu, W. Tang, T. Jiang, F. R. Fan, Y. Pang, L. Chen, Y. Zhang, Z. L. Wang, *Adv. Energy Mater.* **2018**, *8*, 1800889.
[15] J. Yang, F. Yang, L. Zhao, W. Shang, H. Qin, S. Wang, X. Jiang, G. Cheng, Z. Du, *Nano Energy* **2018**, *46*, 220.
[16] H. Qin, G. Cheng, Y. Zi, G. Gu, B. Zhang, W. Shang, F. Yang, J. Yang, Z. Du, Z. L. Wang, *Adv. Funct. Mater.* **2018**, *28*, 1805216.
[17] D. Liu, X. Yin, H. Guo, L. Zhou, X. Li, C. Zhang, J. Wang, Z. L. Wang, *Sci. Adv.* **2019**, *5*, 6437.
[18] Z. L. Wang, A. C. Wang, *Mater. Today* **2019**, *30*, 34.
[19] S. Lin, X. Chen, Z. L. Wang, *Chem. Rev.* **2019**, https://doi.org/10.1021/acs.chemrev.1c00176.
[20] R. Xu, Q. Zhang, J. Y. Wang, D. Liu, J. Wang, Z. L. Wang, *Nano Energy* **2019**, *66*, 104185.
[21] J. Liu, K. Jiang, L. Nguyen, Z. Li, T. Thundat, *Mater. Horiz.* **2019**, *6*, 1020.
[22] J. Liu, M. I. Cheikh, R. Bao, H. Peng, F. Liu, Z. Li, K. Jiang, J. Chen, T. Thundat, *Adv. Electron. Mater.* **2019**, *5*, 1900464.
[23] S. Lin, R. Shen, T. Yao, Y. Lu, S. Feng, Z. Hao, H. Zheng, Y. Yan, E. Li, *Adv. Sci.* **2019**, *6*, 1901925.
[24] X. Huang, X. Xiang, J. Nie, D. Peng, F. Yang, Z. Wu, H. Jiang, Z. Xu, Q. Zheng, *Nat. Commun.* **2021**, *12*, 2268.
[25] J. C. C. Fan, *Sol. Cells* **1986**, *17*, 309.
[26] P. Singh, S. N. Singh, M. Lal, M. Husain, *Sol. Energy Mater. Sol. Cells* **2008**, *92*, 1611.
[27] X. Chen, L. Liu, P. Y. Yu, S. S. Mao, *Science* **2011**, *331*, 746.
[28] L. He, L. C. Wang, H. Sun, J. Ni, Y. Cao, Y. He, K. N. Fan, *Angew. Chem., Int. Ed.* **2009**, *48*, 9538.
[29] Z. Zhang, T. He, J. Zhao, G. Liu, Z. L. Wang, C. Zhang, *Mater. Today Phys.* **2021**, *16*, 100295.
[30] N. Akiya, P. E. Savage, *Chem. Rev.* **2002**, *102*, 2725.
[31] S. Li, J. Nie, Y. Shi, X. Tao, F. Wang, J. Tian, S. Lin, X. Chen, Z. L. Wang, *Adv. Mater.* **2020**, *32*, 2001307.
[32] J. Nie, Z. Ren, L. Xu, S. Lin, F. Zhan, X. Chen, Z. L. Wang, *Adv. Mater.* **2020**, *32*, 1905696.
[33] G. Xue, Y. Xu, T. Ding, J. Li, J. Yin, W. Fei, Y. Cao, J. Yu, L. Yuan, L. Gong, J. Chen, S. Deng, J. Zhou, W. Guo, *Nat. Nanotechnol.* **2017**, *12*, 317.
[34] Z. Zhang, X. Li, J. Yin, Y. Xu, W. Fei, M. Xue, Q. Wang, J. Zhou, W. Guo, *Nat. Nanotechnol.* **2018**, *13*, 1109.
[35] S. Lin, X. Chen, Z. L. Wang, *Nano Energy* **2020**, *76*, 105070.
[36] M. Zheng, S. Lin, Z. Tang, Y. Feng, Z. L. Wang, *Nano Energy* **2021**, *83*, 105810.
[37] F. Yang, M. Zheng, L. Zhao, J. Guo, B. Zhang, G. Gu, G. Cheng, Z. Du, *Nano Energy* **2019**, *60*, 680.
[38] V. R. Stamenkovic, B. S. Mun, M. Arenz, K. J. J. Mayrhofer, C. A. Lucas, G. Wang, P. N. Ross, N. M. T. i. Markovic, *Nat. Mater.* **2007**, *6*, 241.
[39] R. A. Christie, K. D. Jordan, *J. Phys. Chem. B* **2002**, *106*, 8376.
[40] Q. Hu, S. Ouyang, J. Li, Z. Cao, *J. Raman Spectrosc.* **2017**, *48*, 610.
[41] S. Gai, Z. Peng, B. Moghtaderi, J. Yu, E. Doroodchi, *J. Mol. Liq.* **2021**, *333*, 115959.
[42] M. Zhang, E. Lussetti, E. S. Luís, M. P. Florian, *J. Phys. Chem. B* **2005**, *109*, 15060.

